

Profile instabilities of the millisecond pulsar PSR J1022+1001

Michael Kramer^{1,2}, Kiriaki M. Xilouris³, Fernando Camilo⁴, David J. Nice⁵, Donald C. Backer¹,
Christoph Lange², Duncan R. Lorimer^{2,3}, Oleg Doroshenko⁶, Shauna Sallmen¹

ABSTRACT

We present evidence that the integrated profiles of some millisecond pulsars exhibit severe changes that are inconsistent with the moding phenomenon as known from slowly rotating pulsars. We study these profile instabilities in particular for PSR J1022+1001 and show that they occur smoothly, exhibiting longer time constants than those associated with moding. In addition, the profile changes of this pulsar seem to be associated with a relatively narrow-band variation of the pulse shape. Only parts of the integrated profile participate in this process which suggests that the origin of this phenomenon is intrinsic to the pulsar magnetosphere and unrelated to the interstellar medium. A polarization study rules out profile changes due to geometrical effects produced by any sort of precession. However, changes are observed in the circularly polarized radiation component. In total we identify four recycled pulsars which also exhibit instabilities in the total power or polarization profiles due to an unknown phenomenon (PSRs J1022+1001, J1730–2304, B1821–24, J2145–0750).

The consequences for high precision pulsar timing are discussed in view of the standard assumption that the integrated profiles of millisecond pulsars are stable. As a result we present a new method to determine pulse times-of-arrival that involves an adjustment of relative component amplitudes of the template profile. Applying this method to PSR J1022+1001, we obtain an improved timing solution with a proper motion measurement of -17 ± 2 mas/yr in ecliptic longitude. Assuming a distance to the pulsar as inferred from the dispersion measure this corresponds to an one-dimensional space velocity of 50 km s^{-1} .

¹Astronomy Department, University of California, Berkeley, CA 94720, USA

²Max-Planck-Institut für Radioastronomie, Auf dem Hügel 69, 53121 Bonn, Germany

³National Astronomy and Ionosphere Center, Arecibo Observatory, P.O. Box 995, Arecibo, PR 00613, USA

⁴Nuffield Radio Astronomy Laboratories, Jodrell Bank, Macclesfield, Cheshire SK11 9DL, England; Marie Curie Fellow

⁵Joseph Henry Laboratories and Physics Department, Princeton University, Princeton, NJ 08544, USA

⁶Astro Space Center of P.N. Lebedev Physical Institute, Academy of Science, Leninski pr. 53, Moscow 117924, Russia

Subject headings: Pulsars: millisecond pulsars – normal pulsars – profile stability – precession – mode changing – timing precision – PSRs J1022+1001, 1730–2304, B1821–24, J2145–0750

1. Introduction

The discovery of millisecond pulsars (MSPs, Backer et al. 1982), opened new ways to study the emission mechanism of pulsars. Although pulse periods and surface magnetic fields are several orders of magnitude smaller than those of slowly rotating (‘normal’) pulsars, the emission patterns show some remarkable similarities (Kramer et al. 1998, hereafter KXL98; Xilouris et al. 1998, hereafter XKJ98; Jenet et al. 1998). This suggests that the same emission process might work in both types of objects despite orders of magnitude difference in the size of their magnetospheres. A systematic study of the emission properties of MSPs and a comparison of the results with characteristics of normal pulsars can thus lead to new important insight in the emission physics of pulsars. In this paper we investigate unexpected profile instabilities seen for some MSPs and compare them to profile changes known for normal pulsars.

The profile changes described here have consequences for high precision timing of MSPs, in which integrated profiles are cross-correlated with a standard template to measure pulse times of arrival. This procedure implicitly assumes that the shape of the integrated profile does not vary. This premise has never been tested thoroughly for MSPs. The only systematic search we are aware of was an analysis of the planet pulsar PSR B1257+12 which was searched, unsuccessfully, for shape changes (Kaspi & Wolszczan 1993).

Recently, Backer & Sallmen (1997) noticed a significant change in the profile of the isolated millisecond pulsar PSR B1821–24 in about 25% of all observations on time scales of a few hours and possibly days. Even earlier Camilo (1995) described observations of PSR J1022+1001 which show profile changes on apparently shorter time scales, i.e. hours or less. These are the first cases in which such instabilities of profiles averaged over many pulse periods have been reported.

The plan of the paper is as follows. After briefly reviewing what is known about the profile stability of normal pulsars in the next section, we present observations of PSR J1022+1001 and investigate a large data set with respect to pulse shape changes in time, frequency and polarization. In Sect. 3.5 we study the consequences for high precision timing and present a method to compensate for the profile changes when measuring pulse times-of-arrival. Possible explanations for the observed profile changes are discussed in Sect. 4, in view of additional sources showing a similar phenomenon. A summary of this work is made in Sect. 5.

2. Profile stability of normal pulsars

Since the discovery of pulsars it has been known that individual pulses are highly variable in shape and intensity. Nevertheless, summing a sufficiently large number of pulses leads generally to a very stable pulse profile. Systematic studies of the stability of integrated profiles were carried out by Helfand, Manchester & Taylor (1975) and recently by Rankin & Rathnasree (1995). These studies show that a number of a few thousand pulses added together are very often enough to produce a final stable waveform which does not differ from a high signal-to-noise ratio (S/N) template by more than 0.1% or even less.

Despite this stability of pulse profiles, a small sample of normal pulsars shows distinct pulse shape changes on time scales of minutes. This behaviour was first noticed by Backer (1970) and is nowadays well known as *mode changing*. In a mode change the pulsar switches from one stable profile to another on a time scale of less than a pulse period, remains in that mode for typically hundreds of periods, before it returns back to the original pulse shape or switches to another mode. This immediate switch from one mode to the next is a common phenomenon and is often associated with a sudden change in pulse intensity (Rankin 1986). Interestingly, Suleymanova, Izvekova & Rankin (1996) report that a mode switch in PSR B0943+10 is preceded by a decline in intensity for one mode, although again a so called “burst” and “quiet” mode can be distinguished.

Rankin (1986) noted that mode-changing is often observed for such sources which exhibit rather complex profiles showing both the so-called “cone” and “core” components (cf. Rankin 1983; Lyne & Manchester 1988). The mode changing manifests itself as a reorganization of core and cone emission and thus usually affects the *whole profile* (often including polarization properties) rather than only certain pulse longitudes. A rare counter-example might be PSR J0538+2817 (Anderson et al. 1996).

A phenomenon related to mode changing might be *nulling*, i.e. the absence of any pulsed emission for a certain number of periods. There are no clear and unequivocal explanations for the origin of nulling or mode changing which is normally interpreted as a re-arrangement in the structure of the emitting region. Some studies report a possible relationship between mode changing and change in emission height (e.g. Bartel et al. 1982). Other interpretations invoke a large variation in the absorption properties of the magnetosphere above the polar cap (e.g. Zhang et al. 1997). In any case, mode changing will increase the number of pulses that must be added before reaching a final waveform. However, even for pulsars which show mode changes a maximum number of $\sim 10^4$ pulses is typically sufficient for a stable average pulse shape to emerge from the process of adding seemingly random pulses (Helfand, Manchester & Taylor 1975; Rankin & Rathnasree 1995). In contrast, the profile changes of PSR J1022+1001 which we study in this paper, are on much longer time scales, i.e. hundreds of thousands of periods or more as discussed below.

3. The changing profile of PSR J1022+1001

Soon after the discovery of PSR J1022+1001 (Camilo et al. 1996), we included it as part of our regular timing programme at Effelsberg. The first high S/N profile was obtained in 1994 August (Fig. 1a). Comparison with another high S/N profile in 1994 October (Fig. 1b) clearly demonstrated that the resolved pulse peaks differ significantly in their relative amplitudes. Observations at other telescopes confirmed this result which will be discussed in detail in the following.

3.1. Observations and data reduction

The majority of the data presented in this paper were obtained at 1410 MHz with the Effelsberg 100-m radiotelescope of the Max-Planck-Institut für Radioastronomie, Bonn, Germany. Besides the Effelsberg Pulsar Observing System (EPOS) described by KXL98, we also made measurements with the Effelsberg-Berkeley-Pulsar-Processor (EBPP) — a coherent de-disperser that has operating in parallel with EPOS since 1996 October.

The EBPP provides 32 channels for each polarization with a total bandwidth of up to 112 MHz depending on observing frequency, dispersion measure and number of Stokes parameters recorded. For PSR J1022+1001 a bandwidth of 56 MHz can be obtained when recording only the two orthogonal (left- and right hand) circularly polarized signals (LHC and RHC). In polarization mode, i.e. also recording the polarization cross-products, a bandwidth of 28 MHz can be used. Each channel is coherently de-dispersed on-line (assuming a dispersion measure of $DM = 10.25 \text{ pc cm}^{-3}$) and folded with the topocentric pulse period. Individual sub-integrations typically last for 2 min, before they are transferred to disk. A more detailed description of the EBPP can be found in Backer et al. (1997) and Kramer et al. (1999).

In order to monitor the gain stability and polarization characteristics of the observing system, we also performed regular calibration measurements using a switchable noise diode. The signal from this noise diode is injected into the waveguide following the antenna horn and was itself compared to the flux density of known continuum calibrators during regularly performed pointing observations. Switching on the noise diode regularly after observations of pulsars allowed monitoring of gain differences in the LHC and RHC signal paths. Use of this procedure, along with parallel observations by two independent data acquisition systems, allows us to exclude an instrumental origin of the observed profile changes. As a demonstration we show a three hour observation of PSR J1022+1001 in Fig. 2, where each profile corresponds to an integration time of about 40 min. The total power profile (right column) was obtained after appropriately weighting and adding the LHC and RHC profiles shown in the first two columns. In order to guide the eye, we have drawn a dashed horizontal line at the amplitude of the trailing pulse peak, which was normalized to unity. Error bars are based on a *worst-case* analysis, combining 3σ values calculated from off-pulse data with the (unlikely) assumption that the gain difference has (still) an uncertainty of about 20%. Inspecting the time evolution of the shown profiles, we see that the RHC profile remains unchanged

during the whole measurement. At the same time the LHC profile undergoes clear changes. At the beginning of the observations, the trailing pulse peak is the dominant feature in the LHC profile, it then weakens gradually with time, until it becomes of equal amplitude to the first pulse peak. The resulting (total power) profiles reflect exactly this trend.

The measurement presented in Fig. 2 clearly demonstrates that the observed profile changes are not of instrumental origin, owing to the lack of any instrumental effect which could explain the shown evolution on the observed short time scales. Moreover, a correlation between profile shape and source elevation or hour angle is not present. We also searched for a possible relation between profile changes and pulse intensity. In Fig. 2 we thus indicate the flux density measured for the corresponding profiles (with an estimated uncertainty of less than 10%). Clearly, the profile changes are uncorrelated with changes in intensity. Instead, the observed intensity change is presumably caused by interstellar scintillation – a common phenomenon seen in low dispersion measure pulsars (Rickett 1970).

3.2. Profile changes with time

A simple comparison of measured pulse profiles normalized to each of the two pulse peaks provides first clues as to whether the profile is changing as a whole or stable parts are present. In Fig. 3 we present pulse profiles obtained at 1.410 MHz at different epochs. Normalizing to the leading pulse peak, the profile apparently changes over all pulse longitudes, i.e. including the depth of the saddle region and the width of the profile itself. Normalizing the same profiles to the trailing pulse peak seems to cause mainly changes in the first profile part while the trailing one remains stable. The picture seems also to apply to the 430-MHz data obtained by Camilo (1995) and can be confirmed, as discussed later, by the timing behaviour of this pulsar.

Although our data sometimes suggest that variations on time scales of a few minutes are present, we need higher S/N data to confirm this impression. Instead, we reliably study here profile variations visible on longer time scales by adding about $6 \cdot 10^4$ to $8 \cdot 10^4$ pulses each (i.e. 10 to 16 min). Although this corresponds to a much larger number of pulses than needed to reach a stable profile for normal pulsars even in the presence of moding (cf. Sect. 2), we still observe a *smoothly varying* set of pulse shapes. In order to demonstrate that the involved time scales are highly variable, we calculated the amplitude ratio of the leading and trailing pulse peaks at 1410 MHz as the most easily accessible parameter to describe the profile changes. In order to use a large homogeneous data set, we analyzed EPOS data, which were obtained with a bandwidth of 40 MHz, a time resolution of $25.8 \mu\text{s}$ (cf. KXL98) and an integration time as quoted above. We estimated uncertainties in the amplitude ratio using the same worst-case analysis as described before. The mean value of the component ratio (amplitude of the leading pulse peak divided by that of the second one) for the whole data set covering about four years of observations is 0.975 ± 0.009 . Two examples of observations of comparable duration are shown in Fig. 4 where we plot the amplitude ratio as a function of time. During the first measurement the profile appears

to be stable. In the second observation profile changes are evident. This is consistent with the results of an unsuccessful search for periodicities or typical time scales in the amplitude ratio data by computing Lomb periodograms of the unequally sampled data set. Using a method described by Press et al. (1992) we investigated time scales ranging from several hours, over days to months without obtaining significant results.

In order to model the profile changes in detail, we fit the integrated profiles to a sum of Gaussian components, defined as

$$I(\phi) = \sum_{i=1}^n a_{3i-2} \exp \left\{ - \left(\frac{\phi - a_{3i-1} - \phi_0}{a_{3i}} \right)^2 \right\}, \quad (1)$$

where ϕ_0 is a fiducial point. As shown by KXL98 PSR J1022+1001 is well described by a sum of $n = 5$ components (cf. Fig. 5). We applied this method to the whole data set, varying amplitude, positions, and widths of the components. We then developed a model using the median values of component position and width, and found that, surprisingly, this model fits *all* observed profiles well with only adjustments to the relative amplitudes of the components. Of the profiles studied, only 5% of the fits would have been rejected by the criteria of Kramer et al. (1994). According to these, the significance level of the null-hypothesis that the post-fit residuals in the on-pulse region and the data in an off-pulse region of similar size are drawn from the same parent-distribution, must not be less than 95%. Most of the rare cases, where these criteria were not fulfilled, were profiles with very high S/N, indicating a refined model would be needed to perfectly describe the best data.

The summarized results of our Gaussian fitting procedure are presented as a set of histograms in Figures 6 and 7 and Table 1. Figure 6 shows the occurrence of amplitudes for each of the five components (for a numbering see Fig. 5). All profiles were normalized to the trailing peak of the profile, so that the amplitude of the fifth component is always close to unity. Whilst the range of amplitudes is well confined for the first component, the amplitudes for the second and fourth component show a broad distribution. In particular the amplitudes of the third component exhibit a large scatter which is also demonstrated by the summary of the results in Table 1. Inspecting Fig. 5, it is clear that the amplitude, p , of the first pulse peak is made up by a combination of intensities from component 2 and 3, scaling as $p = 0.75a_4 + 0.95a_7$. The quantity p is also displayed in Fig. 6, showing a very broad distribution reflecting the observed changes in amplitude ratio.

We can now test numerically as to whether only parts of the leading profile are changing by repeating the above analysis, but this time allowing additionally for a fit in the relative spacing of the components. The intriguing result is presented in Fig. 7, which shows the distributions of the resulting centroids (relative to the fiducial point) for each component, and Table 1. Interestingly, the scatter in the central position gradually decreases from the leading to the trailing part. At the same time, the corresponding amplitude histogram is almost identical to Fig. 6 (not shown). This result indeed suggests that the trailing part of the profile is more stable than the leading one, which

undergoes significant profile changes.

3.3. Profile changes with frequency

Although profiles of normal pulsars are well known to change significantly with observing frequency, MSPs show often a much smaller profile development (XKJ98). In contrast, the profiles of PSR J1022+1001 show strong changes with frequency, which are inconsistent with the canonical behaviour of normal pulsars (cf. Rankin 1983, Lyne & Manchester 1988).

3.3.1. Large frequency scale

Comparing the *average* pulse profiles of PSR J1022+1001 over a wide range of frequencies (cf. Sayer, Nice & Taylor 1997, Camilo et al. 1996, Kijak et al. 1997, Sallmen 1998, KXL98, Kramer et al. 1999) it becomes clear that profile changes at frequencies other than 400 or 1400 MHz are more difficult to recognize (but nevertheless possible). Only around these two frequencies both prominent pulse peaks are of comparable (although nevertheless changing) amplitude. It has to be addressed by simultaneous multi-frequency observations as to whether the profile changes at different frequencies occur simultaneously. This might, however, be a difficult task given the discovered phenomenon discussed below.

3.3.2. Small frequency scale

For almost all cases, EPOS and EBPP, both operating in parallel, yielded identical pulse profiles. However, at a few occasions the EBPP profiles differed slightly from those obtained with EPOS. The causes are discovered profile variations across the observing bandpass: while EPOS always uses a fixed bandwidth of 40 MHz, the bandwidth of the EBPP for PSR J1022+1001 at 1410 MHz is 56 MHz in total power mode and 28 MHz in polarization mode. When profile changes happen on frequency intervals smaller than this, the obtained profile depends on the exact location and size of the bandwidth used. This is what we observe as demonstrated by a contour plot (Fig. 8), where we show the intensity as a function of pulse longitude and observing frequency. In order to produce this plot we have added 12 min of EBPP total power data folding with the topocentric pulse period. From 30 frequency channels (or 52.5 MHz, i.e. two channels were excised due to technical reasons) each two adjacent ones were collapsed to produce a reliable S/N ratio. All resulting 15 profiles were normalized to the second pulse peak, indicated by the dashed vertical line at 60° longitude. Contour levels were chosen such that solid lines reflect an increase of 3σ (computed from off-pulse data) from the unit amplitude of the trailing pulse peak. Conversely, the dotted lines denote 3σ decreases with respect to the trailing pulse peak. Additionally, we overlay a sample of corresponding profiles as insets whose vertical position reflects their actual observing frequency.

Their horizontal position is arbitrarily chosen for reasons of clarity. The longitude ranges covered in the contour plot and the pulse profiles are identical. Evidently, a significant profile change is occurring on a small frequency scale of the order of 8 MHz, which however also varies for different observations.

Obviously, the profile observed over a large bandwidth is an average of the individual profiles within the band. Depending on the relative occurrence and strength of the various pulse shapes, which is additionally modulated by interstellar scintillation, a whole variety of pulse shapes and time scales can be created.

3.4. Polarization structure

The polarization of PSR J1022+1001 has been already discussed by XKJ98 (see also Sallmen 1998 and Stairs 1998). Here we concentrate on the impact of the profile changes on the polarization characteristics, since it is already clear from Fig. 2 that some changes are to be expected. In Fig. 9 we present polarization data obtained with the EBPP at 1410 MHz for two typical pulse shapes. In the left panel the leading pulse peak is weaker, whereas in the right panel the amplitude ratio is reversed. The linearly polarized intensity (and thus its position angle) is very similar in both measurements, but the circular polarization shows distinct differences. In the right profile we observe significant circular power with positive sense, coinciding with the leading resolved peak of the pulse profile. This feature of circular polarization is not present in the left profile. Similarly, the saddle region of the right profile shows a dip in circular power, while at the same longitude the left profile shows significant circular power with negative sense. Since the position angle swing appears to be identical in both measurements, it rules out some obvious effects due to changes in the viewing geometry. In fact, the strange notch appearing at the maximum of circular power is prominent in both profiles and seems to describe a *resolvable* jump by about ~ 70 deg above the otherwise fairly regular S-like swing. We stress, that the two profiles shown in Fig. 9 represent only two typical pulse profiles. Various states between two extremes can be observed.

The Gaussian components used to model the profile show a distinct correspondence to the polarization structure: the first component coincides with the unpolarized leading part of the profile. The second component corresponds to the first linearly polarized feature, whilst the third component resembles the first large peak in circular polarization. The fourth component coincides with the second peak in linearly polarized intensity, and the fifth Gaussian clearly agrees with the trailing prominent pulse peak. This correspondence between Gaussian components and polarization features, along with the success of the Gaussian model for the various profiles of this and other pulsars (e.g. Kramer et al. 1994, KXL98), strongly suggests that the Gaussian components have some physical meaning, and are not just a mathematical convenience used to describe profiles.

3.5. Timing solution

We have undertaken timing observations of PSR J1022+1001 at several observatories and several observing frequencies over a span of four years. In many cases the timing measurements were derived from the same data as used in the profile shape study described above. Data were collected at the 300 m telescope at Arecibo⁷ (May to November 1994; 430 MHz), the 100 m telescope at Effelsberg (December 1994 to July 1998; 1400 MHz); the 76 m Lovell telescope at Jodrell Bank (April 1995 to July 1997; 600 and 1400 MHz); and the 42 m telescope at Green Bank (July 1994 to May 1998; 370, 600, and 800 MHz). At each observatory, data were folded with the topocentric pulse period, de-dispersed (on- or off-line), and recorded, along with the observation start time.

Times of arrival were calculated by cross-correlating the data profiles with a standard template. For the Green Bank and Jodrell Bank data, a template with fixed shape was used. For the Arecibo and Effelsberg data, the model of five Gaussian components with fixed width and separation but freely varying amplitudes was used. The Arecibo data were not calibrated (left- and right-hand circular polarizations were summed with arbitrary weights), and systematic trends were evident in the residual arrival times, even after allowing Gaussian component amplitudes to vary. The trends were reduced somewhat by fitting the residuals to a linear function of the amplitudes of the five Gaussian components and removing the resulting function from the data. These procedures had the net effect of reducing the rms residual arrival times from $25\ \mu\text{s}$ to $17\ \mu\text{s}$ for two minute integrations. Still, some systematics remained, typically drifts of order $20\ \mu\text{s}$ over time spans of 2 hours (Figure 10).

An alternative scheme for timing the Arecibo data, in which a conventional fixed-template scheme was used, but only that part of the profile from the central saddle point through the trailing edge were given weight in the fit, gave results very similar to those of the five-Gaussian fit. We view this as further evidence that the trailing edge of the profile is relatively stable, while the leading profile is variable.

A total of 4277 times of arrival (TOA) were measured. These were fit to a model of pulsar spin-down, astrometry, and orbital elements using the TEMPO program. Root-mean-square (RMS) residual arrival times after the fit were of order $15\text{--}20\ \mu\text{s}$ for the Arecibo, Jodrell Bank, and Effelsberg data sets, and $40\text{--}100\ \mu\text{s}$ for the Green Bank data (Figure 11). To partially compensate for systematic uncertainties, the Arecibo TOAs were given uniform weights in the fit (equivalent to a timing uncertainty of $17\ \mu\text{s}$), and systematic terms (of order $10\ \mu\text{s}$) were added in quadrature to the uncertainties of TOAs from other observatories. The resulting fits had reduced χ^2 values close to 1 for each observatory, and the overall fit had a reduced χ^2 of 1.09 for the full data set. Our best estimates of timing parameters are listed in Table 2. To guard against remaining systematic errors, we separately analyzed several subsets of the data and incorporated the spread in parameters thus

⁷The Arecibo Observatory, a facility of the National Astronomy and Ionosphere Center, is operated by Cornell University under a cooperative agreement with the National Science Foundation.

derived into the uncertainties in Table 2. Particular data sets considered included the individual sets from Green Bank, Jodrell Bank, and Effelsberg; a smoothed data set (in which all TOAs from a given day were averaged); and a data set which excluded all earth-pulsar lines-of-sight which passed within 30° of the Sun. We recommend that the uncertainties thus derived be treated as 1σ values.

Because this pulsar is close to the ecliptic, the uncertainty in ecliptic latitude, as determined by timing, is much greater than the uncertainty in ecliptic longitude. To minimize covariance between fit parameters, the pulsar’s position and proper motion are thus best presented in ecliptic coordinates. The ecliptic coordinates given in Table 2 are based on the reference frame of the DE 200 ephemeris of the Jet Propulsion Laboratory, rotated by $23^\circ 26' 21.4119''$ about the direction of the equinox.

The proper motion of this pulsar has not been previously reported. The measured proper motion in ecliptic longitude, μ_λ , translates to a one-dimensional space motion of 50 km s^{-1} , assuming a distance of 0.6 kpc, as inferred from the dispersion measure. This is typical of the velocities of millisecond pulsars (e.g. Lorimer 1995, Cordes & Chernoff 1998).

4. Discussion

For PSR J1022+1001 we clearly demonstrated the existence of highly unusual changes in pulse shape and polarization which cannot be explained by instrumental effects. Studies of other MSPs reveal that PSR J1022+1001 is not the only source for which such behaviour can be observed. Backer & Sallmen (1997) have already discussed a similar phenomenon for PSR B1821–24. Another MSP where we find profile changes is PSR J1730–2304 (see Fig. 12). Its usual weakness at 1410 MHz (cf. KXL98) prevents a data analysis as possible for PSR J1022+1001, but similar profile changes have also been observed at the Parkes telescope (Camilo et al. in prep.). Very recently, Vivekanand, Ables & McConnell (1998) also described small profile changes of PSR J0437–4715 at 327 MHz. Although they observed this highly polarized pulsar only with a single polarization, and although Sandhu et al. (1997) demonstrate that measurements of this pulsar are difficult to calibrate, Vivekanand et al. argue that these pulse variations are real. In any case, the low time resolution of their observed profiles prevents a detailed analysis.

It was already noted by XKJ98 that for some MPSs profile changes can be prominent in the polarization characteristics whereas the total intensity remains mostly unchanged. As an intriguing example we refer to PSR J2145–0750, for which XKJ98 measured at 1410 MHz a high degree of polarization and a well defined, flat position angle (see their Fig. 1). Recent results indicate that for most of the time, the profile seems in fact to be weakly polarized with a highly disturbed position angle swing (Sallmen 1998, Stairs 1998). However, a profile very similar to XKJ98’s 1410 MHz observation has been observed by Sallmen (1998) also at 800 MHz.

As it is apparently the case for PSRs J1022+1001 and B1821–24, only certain parts of the pro-

file seem to actually change. Thus, we can exclude any propagation effect due to the interstellar or interplanetary medium since it should affect all parts of the profile simultaneously. When we compare the properties of this ‘strange’ sample of MSPs, we notice that PSRs J0437–4715, J1022+1001 and J2145–0750 have an orbiting companion while both PSRs J1730–2304 and B1821–24 are isolated pulsars. The existence of a binary companion is therefore certainly unrelated to the observed phenomenon. The pulse periods of the pulsars range from 3.05 ms (PSR B1821–24) to 16.45 ms (PSR J1022+1001), and their profiles are not only vastly different in shape and frequency development (KXL98 and XKJ98), but also dissimilar in their polarization structure (XKJ98). While, for instance, in the cases of PSRs J1730–2304 and B1821–24 a highly linearly polarised component seems to change in intensity, it is a weakly polarised component in the case of PSR J1022+1001.

Another prominent example where profile changes for a recycled pulsar have been noticed, are those of the binary pulsar PSR B1913+16 which were described by Weisberg, Romani & Taylor (1989), Cordes, Wasserman & Blaskiewicz (1990) and Kramer (1998). The observed secular, small change in the amplitude ratio and now also separation of the components is evidently caused by geodetic precession of the neutron star. However, the time scales of the profile changes discussed here are by far shorter and also the amplitudes involved are dramatically larger. In combination with the stable polarization angle swing (at least for PSR J1022+1001), we can certainly exclude a precession effect for the profile changes of our studied sample.

The most simple explanation for the observations would be if we had discovered a mode change as long known for normal pulsars. Although mode changes are not understood even for slowly rotating pulsars, we would not have to invoke previously unknown effects. Comparing the number of normal pulsars known when Backer (1970) discovered mode changing, we note that it is similar to the number of MSPs known now. However, if the profile changes were just another aspect of the mode changing for normal pulsars, we would expect similarly that even in such a case a large number of typically 10^4 pulses should be sufficient to average out any random fluctuation in the individual pulses, i.e. producing a stable waveform. For PSR J1022+1001 this would mean to obtain a non-changing pulse profile already after only 3 min of integration time, in contrast to what is observed, which is a pulse shape changing *smoothly* on much longer time-scales. Besides, except for the case of PSR J0437–4715 reported by Vivekanand et al. (1998), the pulse shape changes discussed here seem to appear only in certain parts of the profile while others are obviously unaffected. This together with the obvious lack of a relation between pulse shape and intensity is unusual for the moding behaviour as seen in slowly rotating pulsars.

Most important, however, is that the ‘classical’ mode changing does not provide an explanation for the extraordinary narrow-band variation of the profile of PSR J1022+1001, which is most reminiscent of a scintillation pattern. Since we excluded propagation effects caused by the interstellar medium, the data could be interpreted as a magnetospheric propagation effect but also in the context of a previously unnoticed narrow-band property of the emission process. The latter would be a surprising result since most of the previous pulsar studies favour a broad band emission process (e.g. Lyne & Smith 1998). We note here that Smirnova & Shabanova (1992) describe

simultaneous observations of PSR B0950+08 at very low frequencies of 60 MHz and 102 MHz. Observing with only one linear polarization they report a previously unnoticed profile change of this source which does not seem to occur at both frequencies at the same time. Similar to our observations, they noticed a narrow-band variation of the pulse profile at both frequencies with a characteristic bandwidth of 30–40 kHz. Arguing that recording only one linear polarization is not responsible for this effect, they also consider a narrow band property of the emission process or a scintillation effect of spatially separate sources of emission. Smirnova & Shabanova favour the latter explanation and give estimates for the separation of the emission regions. Applying similar calculations to our case, we however easily derive differences in emission height which are larger than the light-cylinder radius of PSR J1022+1001.

It is interesting to note that the profile changes of PSR J1022+1001 bear certain similarities to the behaviour of the well known mode-changing pulsar PSR B0329+54 (Bartel et al. 1982). McKinnon & Hankins (1993) pointed out that “gated” pulse profiles of PSR B0329+54 produced by single pulses sorted according to their intensity, revealed a shift in the pulse longitude of the core component depending on its intensity. In order to explain this effect, they considered a different emission height for strong and weak pulses as well as a circular motion of the core component around an axis off-center to the magnetic axis. The profile changes in PSR J1022+1001 could be explained in a similar manner, assuming that a core component moves, for instance, on an annulus whose center is displaced from the magnetic axis but closer to the emission region of the leading pulse peak. Those profiles with an amplitude ratio larger than unity (cf. Sect. 3.2) are then produced when the core component is positioned in such a way that it adds to the observed intensity of the first pulse peak. Most of the time, however, it will be away from the first pulse peak, leading to an average amplitude ratio lower than unity as observed. Since core components are mostly associated with circular polarization rather than linear, this simple picture also provides an explanation why only the circular polarization is changing whereas the linear remains unchanged. A rough estimate for the displacement can be calculated by using Eqn. (5) of McKinnon & Hankins (1993), a lower limit for the magnetic inclination angle α of 60° (XKJ98) and the spacing of the centroids of components 3 and 5 of $\Delta t \sim 0.55\text{ms}$ (Fig. 7). This results in a displacement of $\sim 1.2\text{km}$, which corresponds interestingly to the radius of a dipolar polar cap for PSR J1022+1001. A movement of the core on a circular path would, however, imply a typical time scale for the profile changes, which is not observed. If the motion of the core component happens instead in an irregular manner, obvious time scales might not be present. Nevertheless, fluctuation spectra of observed single pulses may be able to resolve a possible movement of the core. Those results should be frequency independent, since all profile changes should obviously occur simultaneously over a wide range of frequencies. Single pulse studies also offer a chance to detect possible correlations between the intensity of single pulses and the resulting average pulse profile as in the cases of PSR B0329+54 (McKinnon & Hankins 1993) or PSR J0437–4715 (Jenet et al. 1998). We note that a preliminary analysis of recent Arecibo data at 430 MHz suggest that “giant pulses” for PSR J1022+1001 occur – if present at all – much less than once per 10^4 stellar rotations, which is already much less than observed for the Crab pulsar (e.g. Lundgren et al. 1995) or PSR B1937+21 (e.g. Sallmen & Backer 1995;

Cognard et al. 1996).

Although this above simple picture can apparently explain some of the observed features at least qualitatively, it bears the fundamental problem that we still would not know what causes this motion of individual components. The $E \times B$ -drift considered by McKinnon & Hankins (1993) would presumably cause a regular motion. Similarly, the model provides unfortunately no direct explanation of the observed narrow-band variation of the pulse profile. Actually, if we are dealing with the same emission mechanism as for normal pulsars (see KXL98, XKJ98 and Jenet et al. 1998) and if we cannot explain the data by the known moding behaviour, then we are left with a propagation effect in the pulsar magnetosphere. This might be combined with different emission altitudes for different parts of the profile and/or differential absorption properties of the magnetosphere above the polar cap. Indeed, one could interpret the position angle swing of PSR J1022+1001 as the composition of two separate S-swings which are delayed to each other and thus represent (independent) emission from different altitudes. In that case, the “notch” in the swing would mark the longitude where the trailing part of the pulse starts to dominate over the leading one. Applying, however, the model derived by Blaskiewicz, Cordes & Wasserman (1991) to estimate the emission height based on polarization properties, we would derive a negative emission altitude for the trailing profile part. More conventionally we could use the spreads in the centroids, Δt , of the fitted Gaussian components as an estimator for a change in emission height, Δr . A rough estimate is given by $\Delta r = c\Delta t/(1 + \sin \alpha)$, where α is the magnetic inclination angle and c the speed of light (see eg. McKinnon & Hankins 1993). Using the largest spread as found for component 1 (i.e. 0.082 ms, cf. Tab. 1), and again $\alpha = 60^\circ$ (XKJ98), we derive a change of $\Delta r \sim 130$ km. This value is still smaller than the light cylinder radius of 785 km.

Although we can apparently construct a simple phenomenological model which can explain some observations qualitatively, a propagation effect in the pulsar magnetosphere might be still the most probable explanation for the observed phenomena. In conclusion, we believe that this interpretation and the reason for the observed narrow-band variation of the pulse shape should be addressed with future simultaneous multi-frequency observations of these interesting sources. Only such observations have the potential to distinguish between a propagation effect in the pulsar magnetosphere, which can be expected to be frequency dependent, and those involving a reformation of the emitting regions, which should produce frequency independent properties.

5. Summary

Focussing in particular on PSR J1022+1001, we have demonstrated that a sample of MSPs shows distinct and unusual profile changes. We argued that these profile changes are not caused by instrumental effects or represent a propagation effect in the interstellar or interplanetary medium. In fact, we conclude that the observed variations in pulse shapes (in time and frequency) are intrinsic to the pulsars and that they are *not* consistent with the mode changing effect known for normal pulsars.

We have shown that the profile changes can have a significant impact regarding the apparent timing stability of MSPs. We suggest the usual template matching procedure to be extended by allowing for variations of the amplitudes of different profile component. As demonstrated for PSR J1022+1001 this procedure improves the timing accuracy significantly and has led to the first proper motion measurement for this pulsar.

We are indebted to all people involved in the project to monitor millisecond pulsars in Effelsberg, in particular to Axel Jessner and Alex Wolszczan. MK acknowledges the receipt of the Otto-Hahn Prize, during whose tenure this paper was written, and the warm hospitality of the Astronomy Department at UC Berkeley. FC is a Marie Curie Fellow.

REFERENCES

- Anderson S., Cadwell B. J., Jacoby B. A., Wolszczan A., Foster R. S., Kramer M., 1996, *ApJ*, 468, L55
- Backer D. C., Sallmen S. T., 1997, *Astron. J.*, 114, 1539
- Backer D. C., 1970, *Nature*, 228, 1297
- Backer D. C., Kulkarni S. R., Heiles C., Davis M. M., Goss W. M., 1982, *Nature*, 300, 615
- Backer D. C., Dexter M. R., Zepka A., Ng D., Werthimer D. J., Ray P. S., Foster R. S., 1997, *Publ. Astr. Soc. Pacific*, 109, 61
- Bartel N., Morris D., Sieber W., Hankins T. H., 1982, *Astrophys. J.*, 258, 776
- Blaskiewicz M., Cordes J. M., Wasserman I., 1991, *Astrophys. J.*, 370, 643
- Camilo F., 1995, PhD thesis, Princeton University
- Camilo F., Nice D. J., Shrauner J. A., Taylor J. H., 1996, *Astrophys. J.*, 469, 819
- Cognard I., Shrauner J. A., Taylor J. H., Thorsett S. E., 1996, *ApJ*, 457, L81
- Cordes J. M., Chernoff D. F., 1998, *Astrophys. J.*, 515, 315
- Cordes J. M., Wasserman I., Blaskiewicz M., 1990, *Astrophys. J.*, 349, 546
- Helfand D. J., Manchester R. N., Taylor J. H., 1975, *Astrophys. J.*, 198, 661
- Jenet F., Anderson S., Kaspi V., Prince T., Unwin S., 1998, *Astrophys. J.*, 498, 365
- Kaspi V. M., Wolszczan A., 1993, in Phillips J. A., Thorsett S. E., Kulkarni S. R., eds, *Planets Around Pulsars. Astronomical Society of the Pacific Conference Series*, p. 81
- Kijak J., Kramer M., Wielebinski R., Jessner A., 1997, *Astr. Astrophys.*, 318, L63
- Kramer M., 1998, *Astrophys. J.*, 509, 856
- Kramer M., Wielebinski R., Jessner A., Gil J. A., Seiradakis J. H., 1994, *Astr. Astrophys. Suppl. Ser.*, 107, 515
- Kramer M., Xilouris K. M., Lorimer D. R., Doroshenko O., Jessner A., Wielebinski R., Wolszczan A., Camilo F., 1998, *Astrophys. J.*, 501, 270
- Kramer M., Lange C., Lorimer D., Backer D., Xilouris K., Jessner A., Wielebinski R., 1999, in preparation

- Lorimer D. R., 1995, *Mon. Not. R. astr. Soc.*, 274, 300
- Lundgren S. C., Cordes J. M., Ulmer M., Matz S. M., Lomatch S., Foster R. S., Hankins T., 1995, *Astrophys. J.*, 453, 433
- Lyne A. G., Manchester R. N., 1988, *Mon. Not. R. astr. Soc.*, 234, 477
- Lyne A. G., Smith F. G., 1998, *Pulsar Astronomy*. Cambridge University Press
- McKinnon M., Hankins T., 1993, *Astr. Astrophys.*, 269, 325
- Press W. H., Teukolsky S. A., Vetterling W. T., Flannery B. P., 1992, *Numerical Recipes: The Art of Scientific Computing*, 2nd edition. Cambridge University Press, Cambridge
- Rankin J. M., Rathnasree N., 1995, *Astrophys. J.*, 452, 814
- Rankin J. M., 1983, *Astrophys. J.*, 274, 333
- Rankin J. M., 1986, *Astrophys. J.*, 301, 901
- Rickett B. J., 1970, *Mon. Not. R. astr. Soc.*, 150, 67
- Sallmen S., Backer D. C., 1995, in Fruchter A. S., Tavani M., Backer D. C., eds, *Millisecond Pulsars: A Decade of Surprise*. *Astron. Soc. Pac. Conf. Ser. Vol. 72*, p. 340
- Sallmen S., 1998, PhD thesis, University of California at Berkeley
- Sandhu J. S., Bailes M., Manchester R. N., Navarro J., Kulkarni S. R., Anderson S. B., 1997, *ApJ*, 478, L95
- Sayer R. W., Nice D. J., Taylor J. H., 1997, *Astrophys. J.*, 474, 426
- Smirnova T. V., Shabanova T., 1992, *Sov. Astron.*, 36, 628
- Stairs I., 1998, PhD thesis, Princeton University
- Suleymanova S., Izvekova V., Rankin J., 1996, in Johnston S., Walker M. A., Bailes M., eds, *Pulsars: Problems and Progress*, IAU Colloquium 160. Astronomical Society of the Pacific, San Francisco, p. 223
- Vivekanand M., Ables J., McConnell D., 1998, *Astrophys. J.*, 501, 823
- Weisberg J. M., Romani R. W., Taylor J. H., 1989, *Astrophys. J.*, 347, 1030
- Xilouris K., Kramer M., Jessner A., von Hoensbroech A., Lorimer D., Wielebinski R., Wolszczan A., Camilo F., 1998, *Astrophys. J.*, 501, 286
- Zhang B., Qiao G. J., Lin W. P., Han J. L., 1997, *Astrophys. J.*, 478, 313

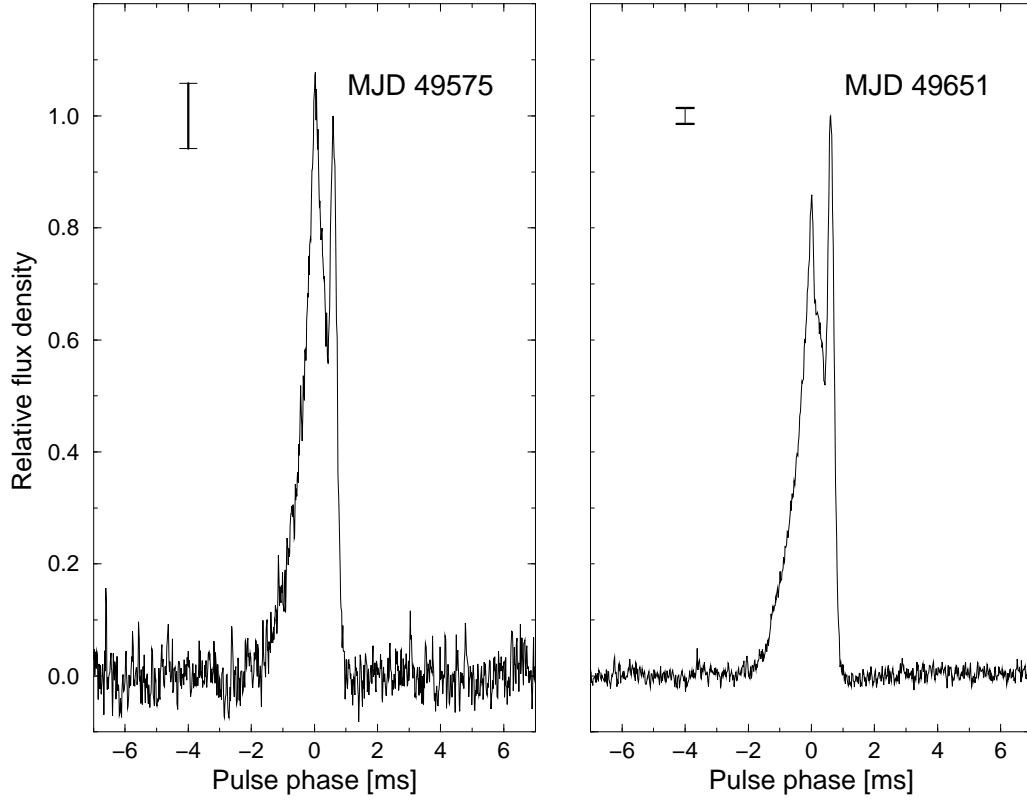


Fig. 1.— Typical profile changes of PSR J1022+1001 as seen during the first measurements obtained in Effelsberg at 1410 MHz. The error bars are conservative, being the result of 3σ values calculated from off-pulse data and a performed worst-case analysis (see text for details). The profiles are significantly different.

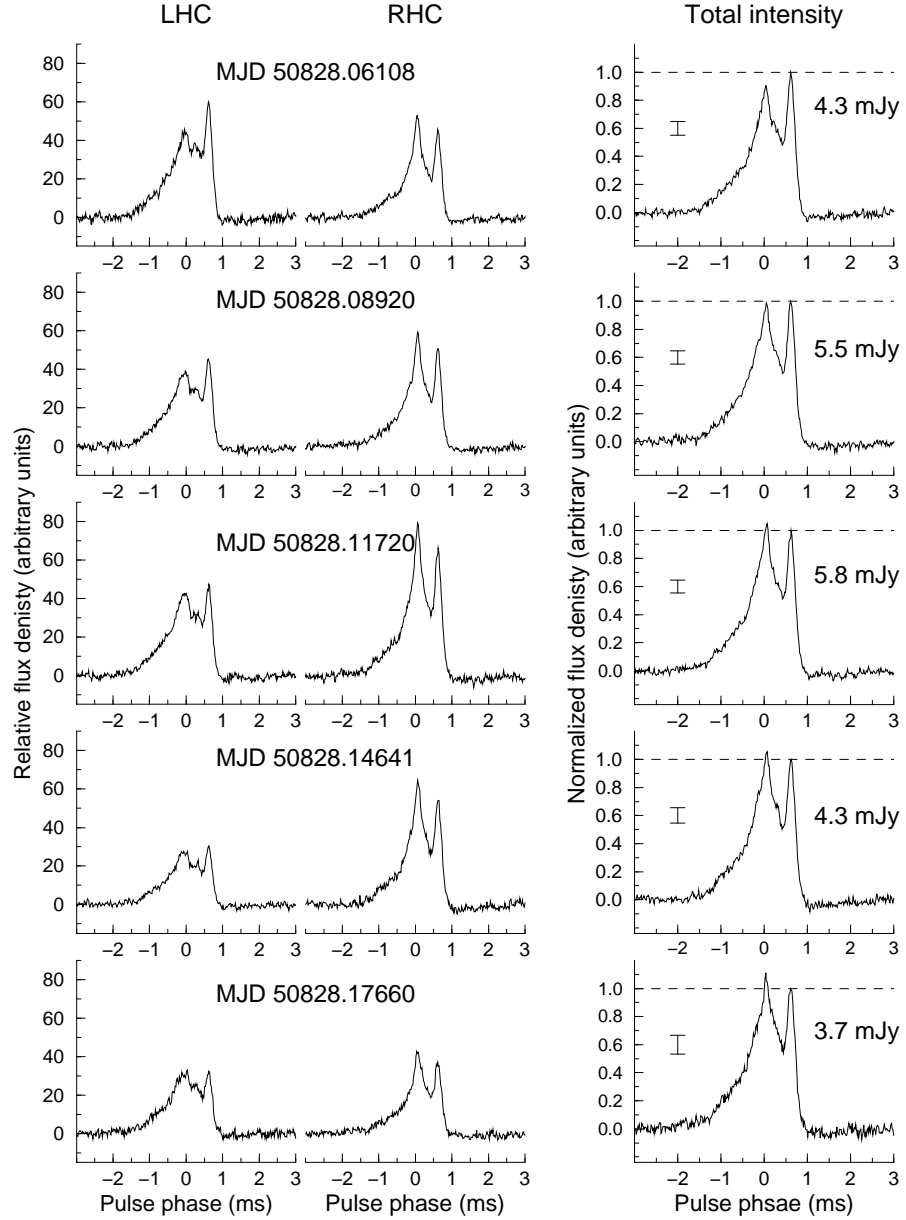


Fig. 2.— Change of integrated profiles for PSR J1022+1001 during a 3.3h observation showing LHC (first column) and RHC (second column) signals and the total power profile (third column) after correctly adding the two polarizations. While LHC and RHC profiles are scaled to the same arbitrary flux units, the total power profiles were scaled to unity amplitude of the trailing pulse peak (dashed horizontal line). The error bars are conservative, being the result of a worst-case analysis (see text for details). Measured flux densities noted for each corresponding profile demonstrate that the profile changes are unrelated to pulse intensity.

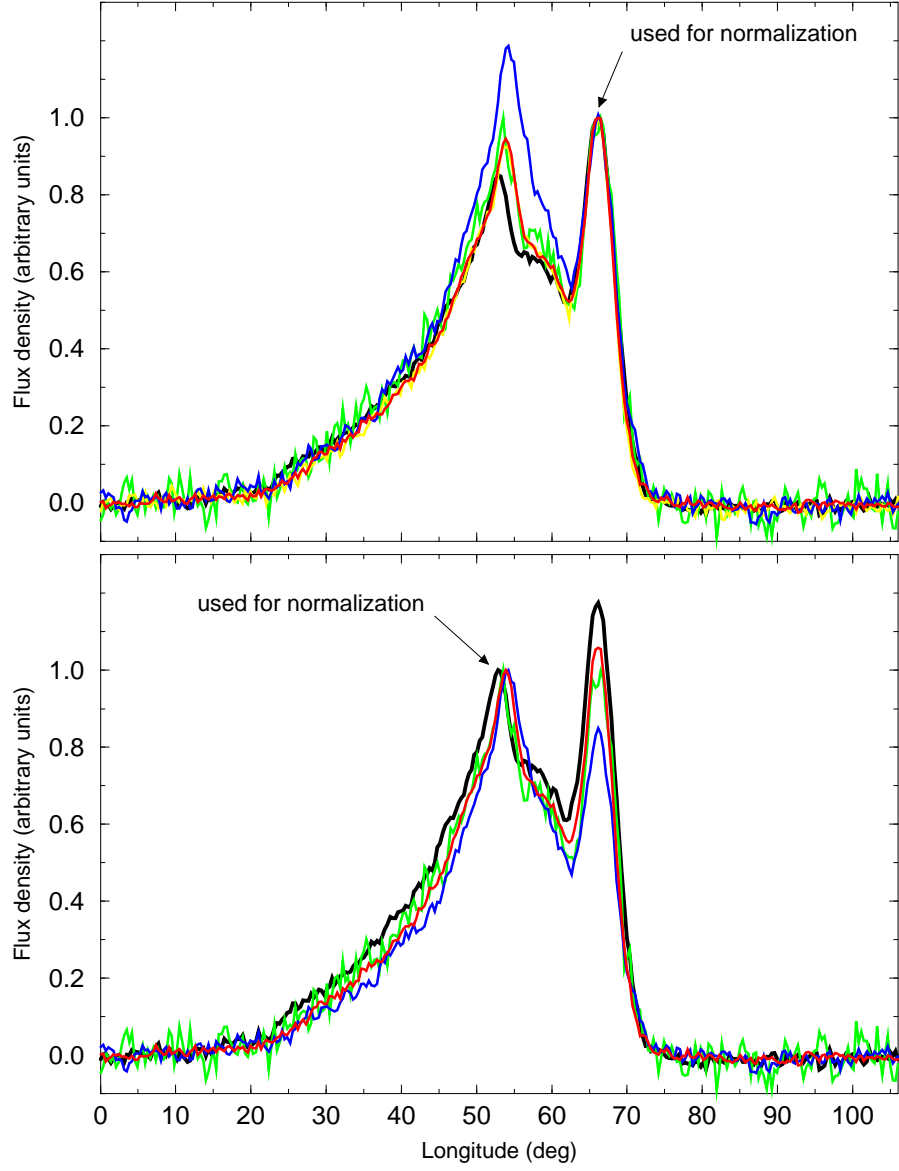


Fig. 3.— Same set of pulse profiles of PSR J1022+1001 observed at 1410 MHz, normalized to the leading (bottom panel) and trailing (top panel) pulse peak.

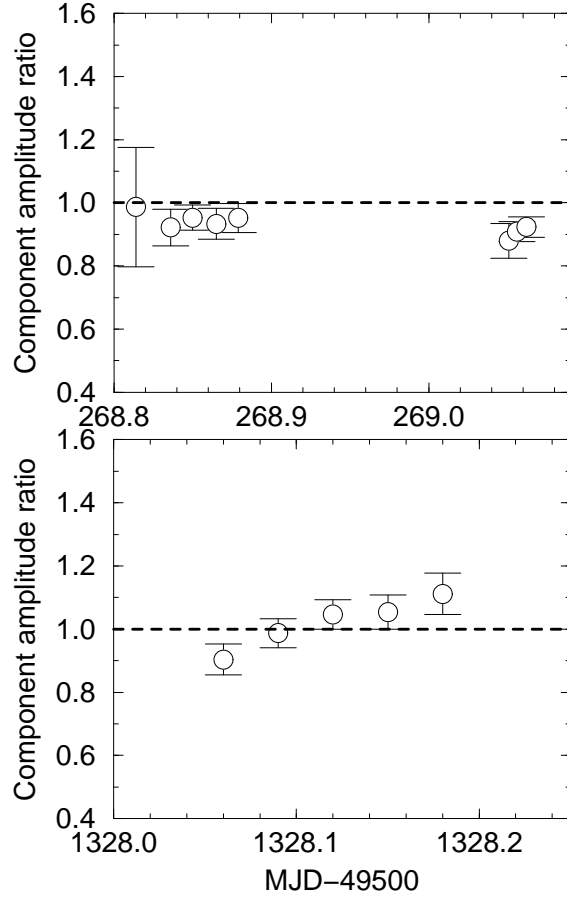


Fig. 4.— Ratio of pulse peak amplitudes (amplitude of leading peak divided by that of trailing one) as a function of time for two different observations of similar length. The difference in the time scale of the profile changes is clearly visible.

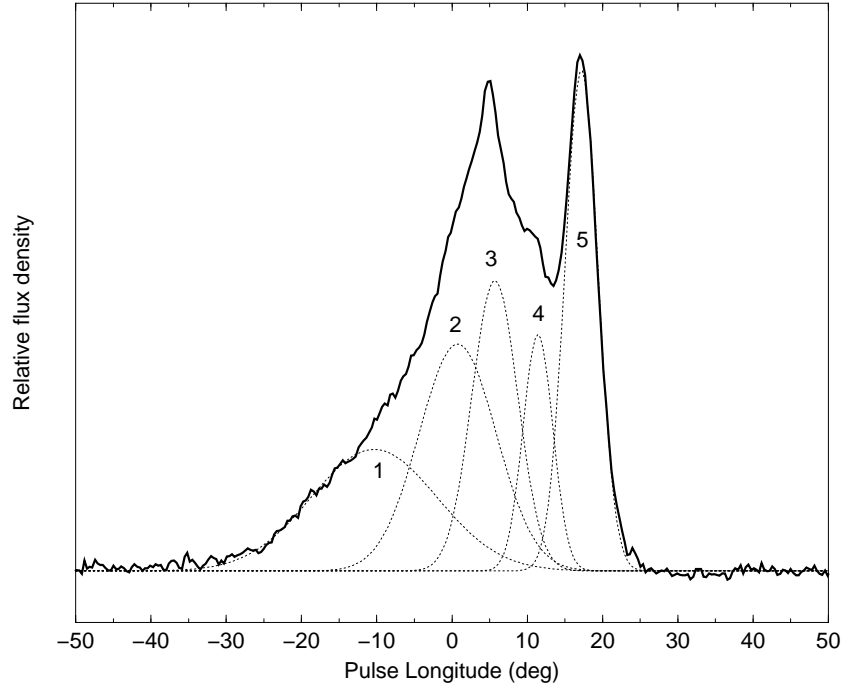


Fig. 5.— Example of a profile observed for PSR 1022+1001 at 1410 MHz separated into five Gaussian components. Adjusting only their relative amplitudes describes all observed different pulse shapes with surprising accuracy.

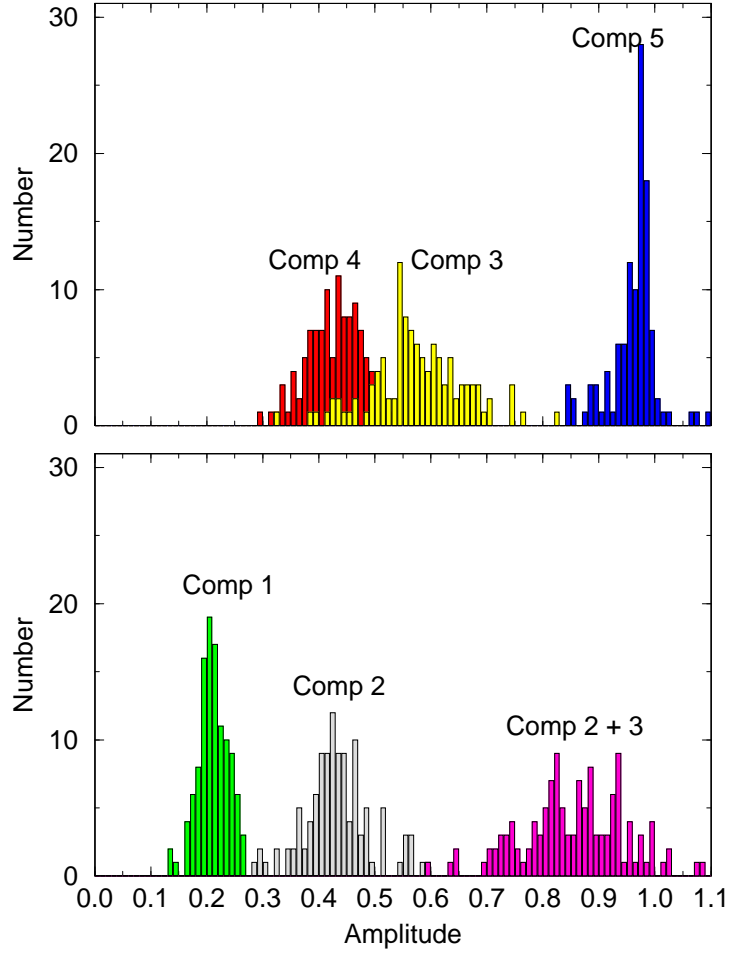


Fig. 6.— Statistical results of fitting a model of five Gaussian components to the profiles observed at 1410 MHz (see text). During these fits only the amplitudes of the Gaussians were adjusted. Obtained amplitude distributions are shown (see Fig. 5 for component numbering). The right distribution in the bottom panel reflects an appropriate linear combination of the second and third component, corresponding to the first pulse peak (see text).

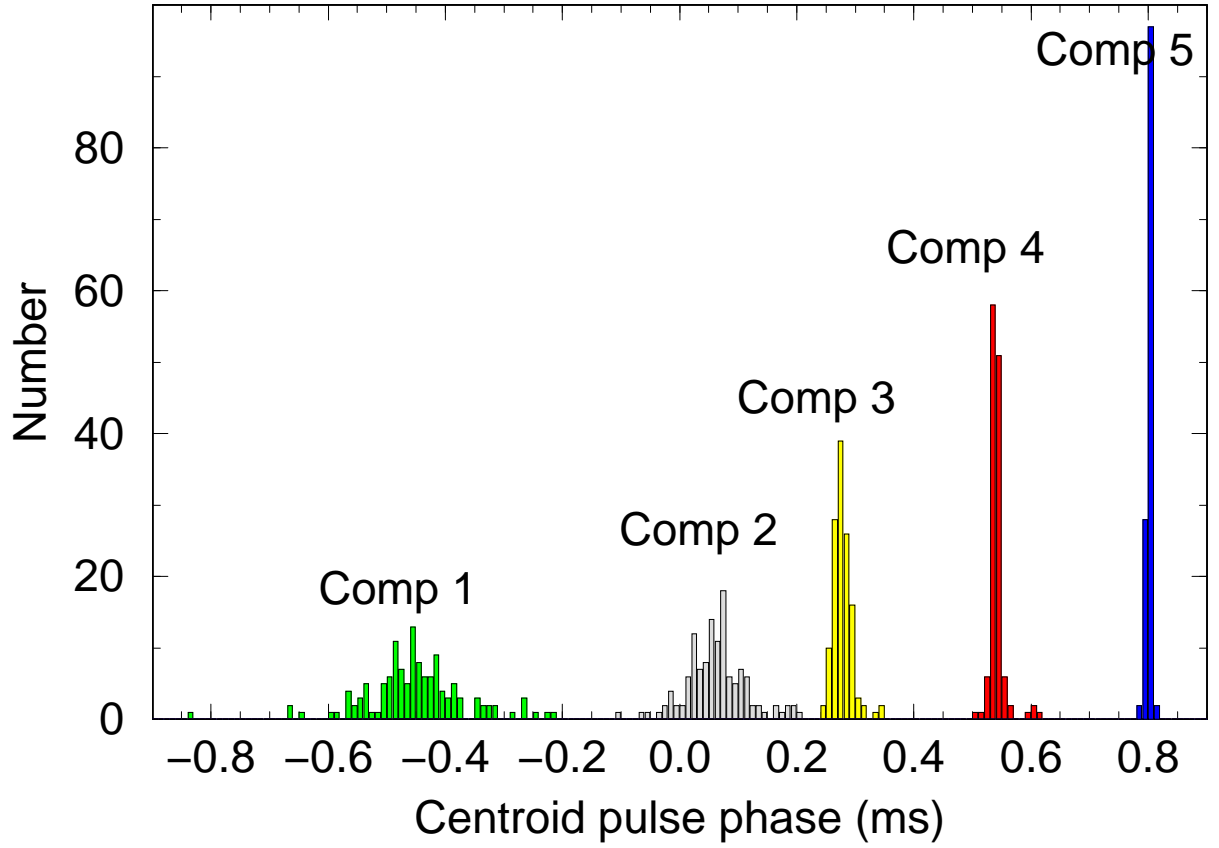


Fig. 7.— Statistical results of fitting a model of five Gaussian components to the profiles observed at 1410 MHz (see text). During these fits the amplitudes and centroids of the Gaussians were adjusted. Obtained centroid distributions are shown (see Fig. 5 for component numbering).

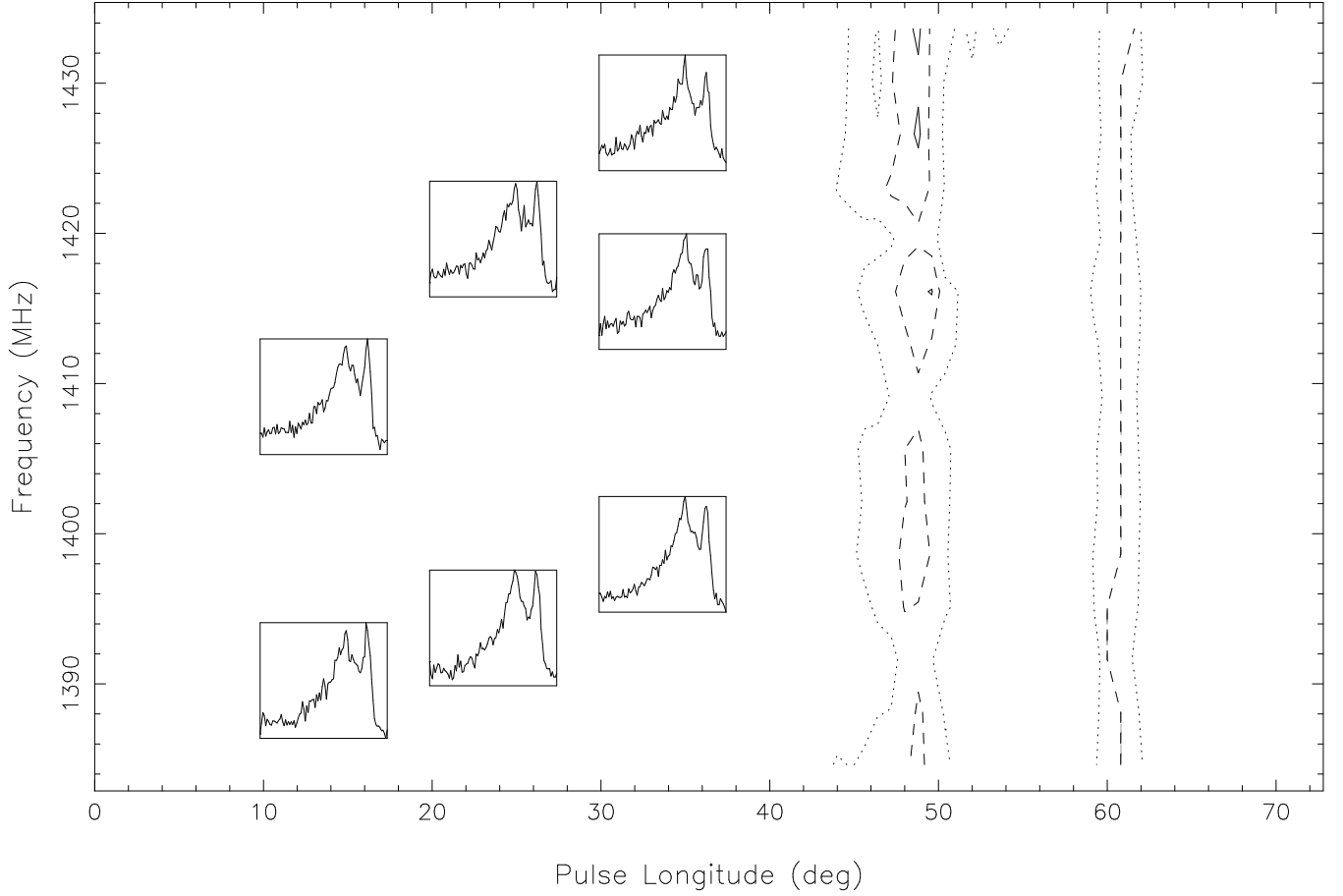


Fig. 8.— Contour plot of pulse intensity as a function of pulse longitude and observing frequency covering a bandwidth of 52.5 MHz centered at 1410 MHz. Solid (dotted) contour lines reflect an increase (decrease) of 3σ from the unit amplitude of the trailing pulse peak (dashed contours). A sample of measured profiles is shown as insets whose vertical position corresponds to their actual observing frequency. The longitude ranges of the contour plot and shown pulse profiles are identical.

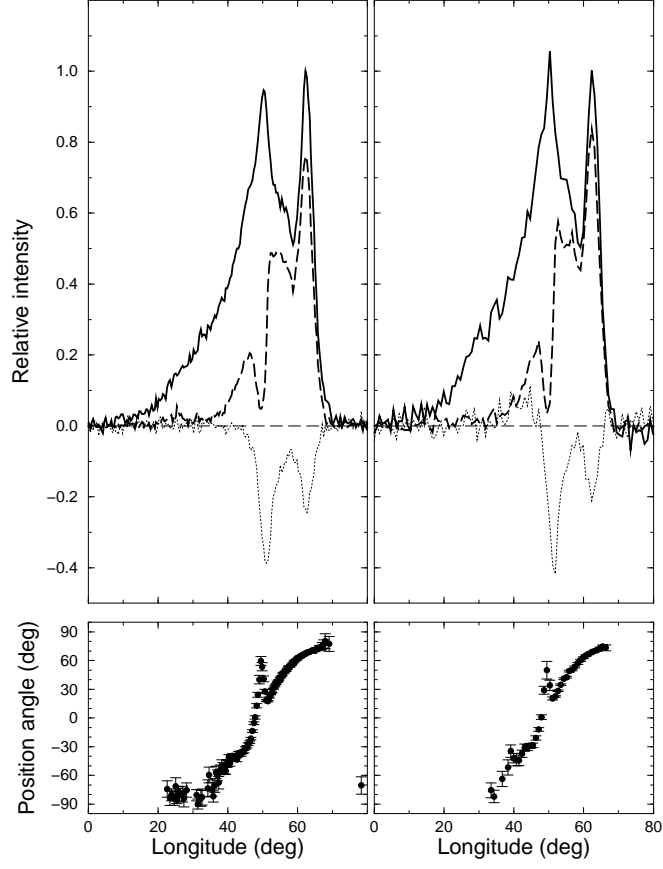


Fig. 9.— Polarization characteristics observed for different pulse shapes at 1410 MHz. While the linear polarization (dashed line) is essentially unchanged, significant differences in circular polarization (dotted line) like a sense reversal at position of the first pulse peak are visible in the right plot while missing on the left.

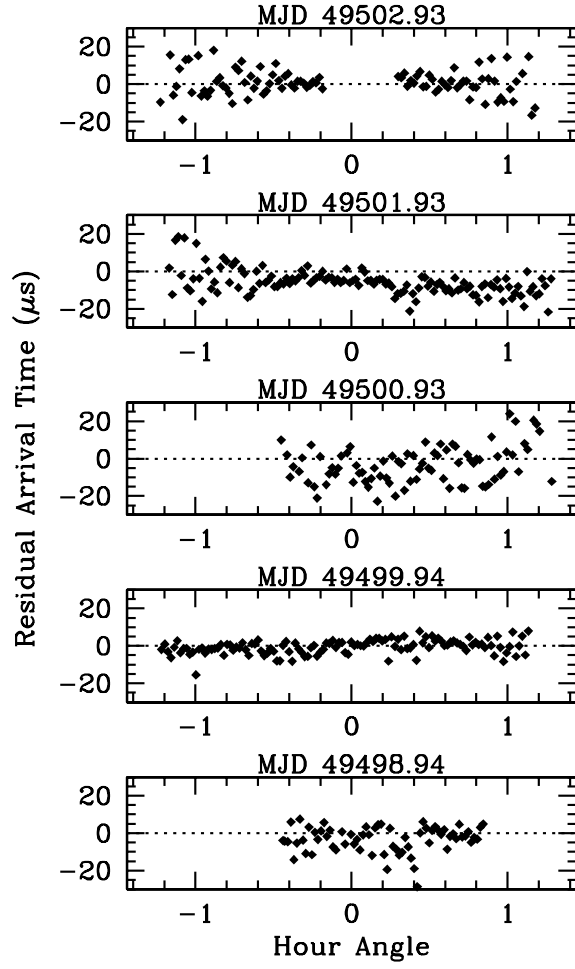


Fig. 10.— Residual arrival times of the first five epochs of Arecibo data. Trends evident in the data include drifts in arrival times as well as overall offsets from zero. As discussed in the text, these artifacts are likely instrumental in nature.

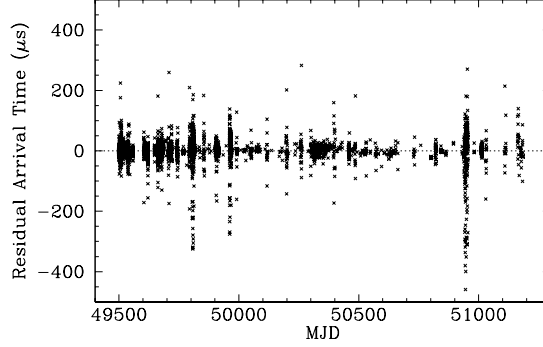


Fig. 11.— Residual arrival times of all data points.

Table 1: Statistical results of fitting a model of five Gaussian components to profiles observed at 1410 MHz. In the first case (second and third column) only the relative amplitudes were adjusted, while in the second also the Gaussian centroids were varied (fourth and fifth column). For the amplitudes, which are quoted in units of the trailing pulse peak, we list variances and their ratio to the mean amplitudes. For the centroids of the components in units of milliseconds (relative to the fiducial point), we quote variances and their values normalized to the (fixed) width of each component.

Comp	Amplitudes		Centroids	
	σ	σ/mean	σ (ms)	σ/width
I.	0.027	0.128	0.082	0.053
II.	0.059	0.134	0.057	0.059
III.	0.090	0.160	0.017	0.031
IV.	0.052	0.122	0.014	0.039
V.	0.042	0.043	0.004	0.009

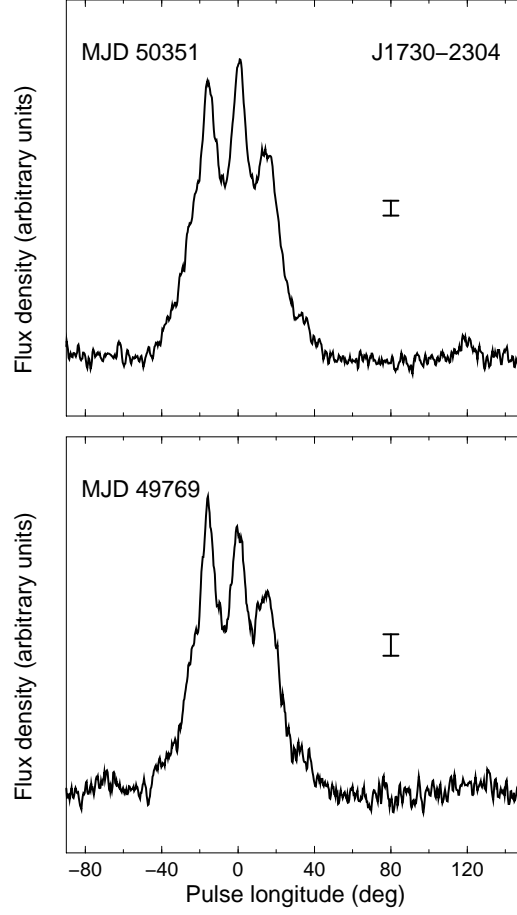


Fig. 12.— Two profiles of PSR J1730–2304 measured in Effelsberg at 1410 MHz at different epochs. Error bars reflect 3σ values calculated from off-pulse data. A clear change in the profile is visible.

Table 2: Timing parameters of PSR J1022+1001. Numbers in parentheses are 1σ uncertainties derived from a combination of all four available data sets.

Ecliptic Longitude, λ (deg)	153.8659226(8)
Ecliptic Latitude, β (deg)	−0.0641(1)
Proper Motion in λ , μ_λ (mas/yr)	−17(2)
Period (ms)	16.4529296832030(4)
Period derivative (10^{-20})	4.341(4)
Epoch of period (MJD)	50250
Dispersion measure ^a (pc cm ^{−3})	10.246
Projected semi-major axis (light s) ...	16.765409(2)
Eccentricity	0.00009735(8)
Time of periastron passage (MJD) ...	50246.716(2)
Orbital Period (days)	7.805130162(6)
Angle of periastron (degrees)	97.67(7)
Right Ascension ^b	10 ^h 22 ^m 57 ^s .997(9)
Declination ^b	10°01′52″.1(3)

^aHeld fixed

^bCalculated from λ and β